The Detection of Mixed Layer Depth and Entrainment Zone Thickness from Lidar Backscatter Profiles

D. G. STEYN

Atmospheric Science Programme, Department of Geography, University of British Columbia, Vancouver, British Columbia, Canada

M. BALDI

Institute for Atmospheric Physics, IFA-CNR, Rome, Italy

R. M. HOFF

Air Quality Research Branch, Atmospheric Environment Service, Egbert, Ontario, Canada

12 May 1998 and 5 November 1998

ABSTRACT

A new method is presented for the extraction of mixed layer depth and entrainment zone thickness from lidar, backscatter ratio profiles. The method is based on fitting a four parameter, idealized profile to observed profiles. Optimization of the fit yields values for mixed layer depth and entrainment zone thickness. Since the fitting procedure is based on the entire measured profile, it has a robustness not found in methods based on critical backscatter or backscatter gradient. The method is tested by application to four measured profiles and three synthetic profiles. The sets of profiles include some that are very demanding because of small mixed layer to upper layer backscatter ratio contrasts, or have plumes of high backscatter imbedded in mixed and upper layers. It is shown that the method is robust and simple to implement, even for a sequence of independent profiles.

1. Introduction

Under convective conditions, the atmospheric boundary layer becomes a mixed layer, characterized by approximately height invariant values for winds and scalar quantities. The mixed layer is capped by an entrainment zone, which provides a transition to the (often stable) lower troposphere (Stull 1988). In this case, the mixed layer depth (MLD) is of primary importance since it determines the volume of atmosphere through which surface emitted pollutants can be diluted, and is also a length scale governing the behavior of the largest scales of boundary layer turbulence (Stull 1988). Also of importance is the magnitude of surface layer and entrainment layer turbulent heat flux densities. The former quantity can be easily measured, while the latter is all but inaccessible. Simple parameterizations of entrainment heat flux are often based on the entrainment zone thickness (EZT) (Driedonks and Tennekes 1984). Knowledge of MLD and EZT is thus important for an understanding of the atmospheric boundary layer.

Corresponding author address: Dr. D. G. Steyn, Atmospheric Science Programme, Department of Geography and Oceanography, 217-1984 West Mall, Vancouver, BC, V6T 1Z2, Canada.
E-mail: douw@geog.ubc.ca

MLD and EZT can, in principle, be determined by measurement of profiles of a variety of atmospheric properties, potential temperature being the most common (Lenschow 1986). One very powerful method for probing the atmospheric boundary layer that is receiving increasing attention in the past decade is based on detection of lidar backscatter from aerosols. This method returns a profile of backscatter ratio, from which values for MLD and EZT must be extracted.

The objective of this work is to present a new scheme for the extraction of MLD and EZT from profiles of lidar backscatter ratio. The method is developed in order to overcome arbitrariness, subjectivity, and instabilities in commonly used methods. The intention is to develop a method so robust that it can be applied in an automated scheme.

2. The detection of mixed layer structures from lidar backscatter data

a. Existing techniques

Lidar backscatter data may be analyzed by subjective visual inspection to yield boundary layer parameters such as MLD and EZT (Boers et al. 1984; Nelson et al. 1989). Endlich et al. (1979) pioneered automated de-

tection of boundary layer structures, and particularly MLD from lidar backscatter profiles. Their method of detection was based on calculation of the vertical gradient (db/dz) of backscattered energy. Since mixed layer air generally has a higher aerosol burden than air immediately above, a maximum in $-db/dz$ should signal the MLD. This technique is a common means of automated MLD detection from lidar backscatter profiles derived from both ground-based and aircraft-borne instruments (e.g., Hayden et al. 1997; Hoff et al. 1996). Melfi et al. (1985) and Batchvarova et al. (1997) used an automated detection technique based on a critical absolute backscatter value to detect the transition between lower troposphere and MLD. More recently, wavelet analyses using a Haar wavelet as the mother function have been employed for automatic detection of MLD from aircraft-borne lidar backscatter profiles (Cohn et al. 1997; Davis et al. 1997). Techniques for automated detection of MLD from lidar data mentioned above suffer from a particular set of weaknesses described below.

Techniques based on $-db/dz$ are difficult to implement because of the amplification of noise resulting from the finite difference estimation of the derivative in noisy data. The resulting $-db/dz$ profile is often so noisy that no maximum is evident. Successful implementation of this approach requires averaging of adjacent sets (in time and/or space) of profiles as well as vertical smoothing of the averaged profile. Hayden et al. (1997) averaged 10 adjacent profiles (to yield a horizontal resolution of roughly 2 km) and applied a 5-point running mean (to yield a vertical resolution of roughly 60 m). Obviously, much horizontal and vertical resolution has been lost, and the possibility of spatial bias has been introduced by this averaging. In spite of the averaging and smoothing, the technique still fails to detect the MLD in a disappointingly large number of cases. The $-db/dz$ technique suffers from the frequency with which it will falsely detect the MLD as tops of scattering layers above the true MLD or localized plumes below the true MLD.

Techniques based on critical backscatter are difficult to implement since it is difficult to define a critical backscatter value that distinguishes between boundary layer air and the lower troposphere. Melfi et al. (1985) determine the MLD as the height at which backscatter signal exceeds the clear air value by a small arbitrary, but fixed, value. Clearly the arbitrariness of the choice is a crucial weakness. Batchvarova et al. (1997) attempt to overcome this by defining average backscatter values for both mixed layer and lower troposphere. Their critical backscatter is then the average of these two values. This approach introduces a circularity, since mixed layer average backscatter cannot be defined if MLD is not known. They overcome the difficulty by presetting mixed layer and lower troposphere backscatter based on an analysis of an entire flight leg. The critical backscatter is thus fixed for an entire flight, or even day of operation. The arbitrariness of critical backscatter selection is obviously a weakness of this approach. Two secondary weaknesses arise. Given a critical backscatter (however determined), backscatter values in a given profile are often noisy enough that there is a range of heights within which the critical backscatter is reached, even if the overall backscatter profile consists of a relatively simple increase in backscatter at the mixed layer top. The critical backscatter technique suffers from the frequency with which it will falsely detect the MLD as tops of scattering layers above the true MLD or localized plumes below the true MLD.

b. A new technique

In order to avoid the difficulties outlined above, we turn to an approach that employs the entire backscatter profile. We do this because techniques that utilize the entire backscatter profile should be more robust than those based on that portion of the profile immediately surrounding the MLD. The challenge is to devise a technique that, like wavelet techniques, utilizes the entire profile, yet remains able to detect localized features.

The technique we propose fits an idealized backscatter profile $B(z)$ to the observed backscatter profile $b(z)$ by minimizing a measure of agreement between the two profiles. Clearly $B(z)$ must represent the simplest possible mixed layer, with high backscatter in the mixed layer, and a relatively sharp transition to lower backscatter in air overlying the mixed layer. In a sense, the application of such a method presupposes the backscatter profile of an idealized mixed layer. Alternatively, one could say that such a method will only detect mixed layers with structures that match that particular ideal. One such form of idealized backscatter profile $B(z)$ is

$$B(z) = \frac{(B_m + B_u)}{2} - \frac{(B_m - B_u)}{2}\,\mathrm{erf}\left(\frac{z - z_m}{s}\right), \quad (1)$$

where B_m is the mean mixed layer backscatter, B_u is the mean backscatter in air immediately above the mixed layer, z_m is mixed layer depth, and s is related to the thickness of the entrainment layer. The four idealized backscatter profile parameters are determined by minimizing root-mean-square deviation (rmsd) between $B(z)$ and $b(z)$. An example of this profile form is plotted in Fig. 1. Obviously, the two parameters z_m and s are of major interest. The quantity s represents the thickness of the layer in which mixing between mixed layer air and overlying air is achieved. This so-called entrainment layer (Nelson et al. 1989) is usually defined to be that layer in which the mixing ratio of boundary layer and overlying air lies in the range 0.05–0.95. Ordinates of the error function thus determine that $\mathrm{EZT} = 2.77s$.

A process of multidimensional minimization is needed to find ''best-fit'' values of the profile parameters. Initial attempts to use the downhill simplex method (Press et al. 1992) in multidimensions proved unreliable.

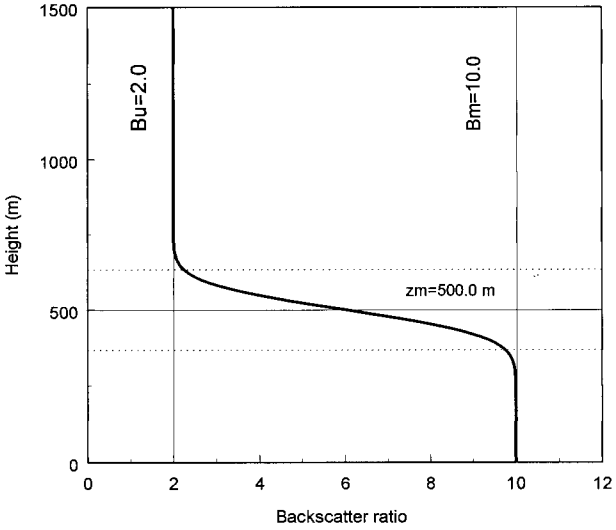

FIG. 1. Idealized backscatter profile with $B_u = 2.0$, $B_m = 10.0$, $z_m = 500.0$ m, and $s = 100.0$ m. The dotted lines indicate the EZT, spanning 277 m centered on an MLD of 500 m.

Implementation of the method of ''simulated annealing'' achieves very satisfactory results with relatively little computational cost. Routines for implementation of this method are described and presented in Press et al. (1992).

3. Application of the technique

The objective of this section is to explore the ability of the MLD and EZT detection scheme described above to detect those quantities in a variety of backscatter profiles. This objective will be achieved by testing the scheme with a range of real and synthetic profiles. The profiles have been selected to represent a range of ''ideal'' conditions, as well as a few profiles whose shape does not conform well to the idealized profile shown in Fig. 1.

a. Testing with real profiles

During a field study (called Pacific '93) of oxidant pollution in the Lower Fraser Valley of British Columbia, Canada (Pottier et al. 1994; Steyn et al. 1997), an aircraft-borne downlooking lidar was operated in a traversing mode from an elevation of roughly 4300 m above sea level for a number of days. The lidar instrument is described in detail in Hoff et al. (1997) and the aircraft program in Hayden et al. (1994). The set of lidar derived backscatter profiles (being one second average with a vertical resolution of roughly 12 m) provides an excellent testing ground for the technique being presented. Four backscatter profiles were selected from those collected during flight P314 on 3 August 1993 between 0849 and 1132 PST. Times and positions of the profiles as well as parameters defining the fitted profiles are shown on Table 1. Locations of the profiles in relation to topography and coastline can be found by reference to Fig. 1 of Steyn et al. (1997). For simplicity, the selected profiles are referred to as P1 to P4. The four fitted profiles and original backscatter profiles are plotted on Figs. 2a–d.

Profile P1 (Fig. 2a) represents a profile that conforms very closely to the ''ideal'' profile shape, apart from a noise component. A simple examination of Fig. 2a shows that the technique has no difficulty in detecting the MLD (as coinciding with the region of sharply changing backscatter) and EZT in this profile.

Profile P2 (Fig. 2b) shows a mixed layer with a deep layer of weakly scattering (and presumably less polluted) air in its lower half. The profile clearly does not conform to the idea of a mixed layer in which all quantities are well mixed in the vertical. Despite the considerable vertical variability of backscatter within the mixed layer, the technique has little difficulty in determining the MLD since it detects the uniform backscatter in the upper layer and the sharp rise in backscatter within the entrainment zone. An examination of a two-dimensional (X–Z) plot of backscatter ratio along this flight leg (L8N on 3 Aug 1993) confirms that the mixed layer around latitude 48.7°N is in the range 520–540 m deep.

Profile P3 (Fig. 2c) contains a shallow plume of moderately scattering air immediately above a shallow mixed layer. While the origin of this layer is not fully confirmed, it is likely that this plume is in the residual layer from the previous day. As with profile P2, this

TABLE 1. Lidar backscatter ratio profiles from 3 Aug 1993 during Pacific '93 field study. The quantities z_{m1}, z_{m2}, and z_{md} are MLD detected by other techniques. Here, z_{m1} and z_{m2} are MLD determined by critical backscatter, the upper height is the first height at which backscatter equals the critical value when scanning the profile downward, the lower height is for upward scanning. Also, z_{md} is MLD detected by the derivative of backscatter. Here, B_u, B_m, z_m and s are defined in Eq. (1), and f is root-mean-square deviation between measured backscatter profile and fitted profile.

Profile	Leg	Lat	Long	Time (PST)	z_{m1} (m)	z_{m2} (m)	z_{md} (m)	B_u	B_m	z_m (m)	s (m)	f
p1	L6N	48.8838	122.515	1031	648	470	552	3.316	12.331	521	105	0.704
p2	L8N	48.7016	122.658	1003	639	402	–*	3.578	11.171	534	111	1.726
p3	L9S	49.0300	122.746	0956	450	189	169**	3.407	13.616	246	87	0.760
p4	L9S	49.0435	122.746	0955	341	163	169**	3.731	22.623	236	112	0.752

* The procedure detected the most significant maximum in $-db/dz$ as that at the surface.

** The procedure was successful in detecting a maximum in $-db/dz$, but returned a result, which appears to be related to features within the mixed layer, rather than at the top.

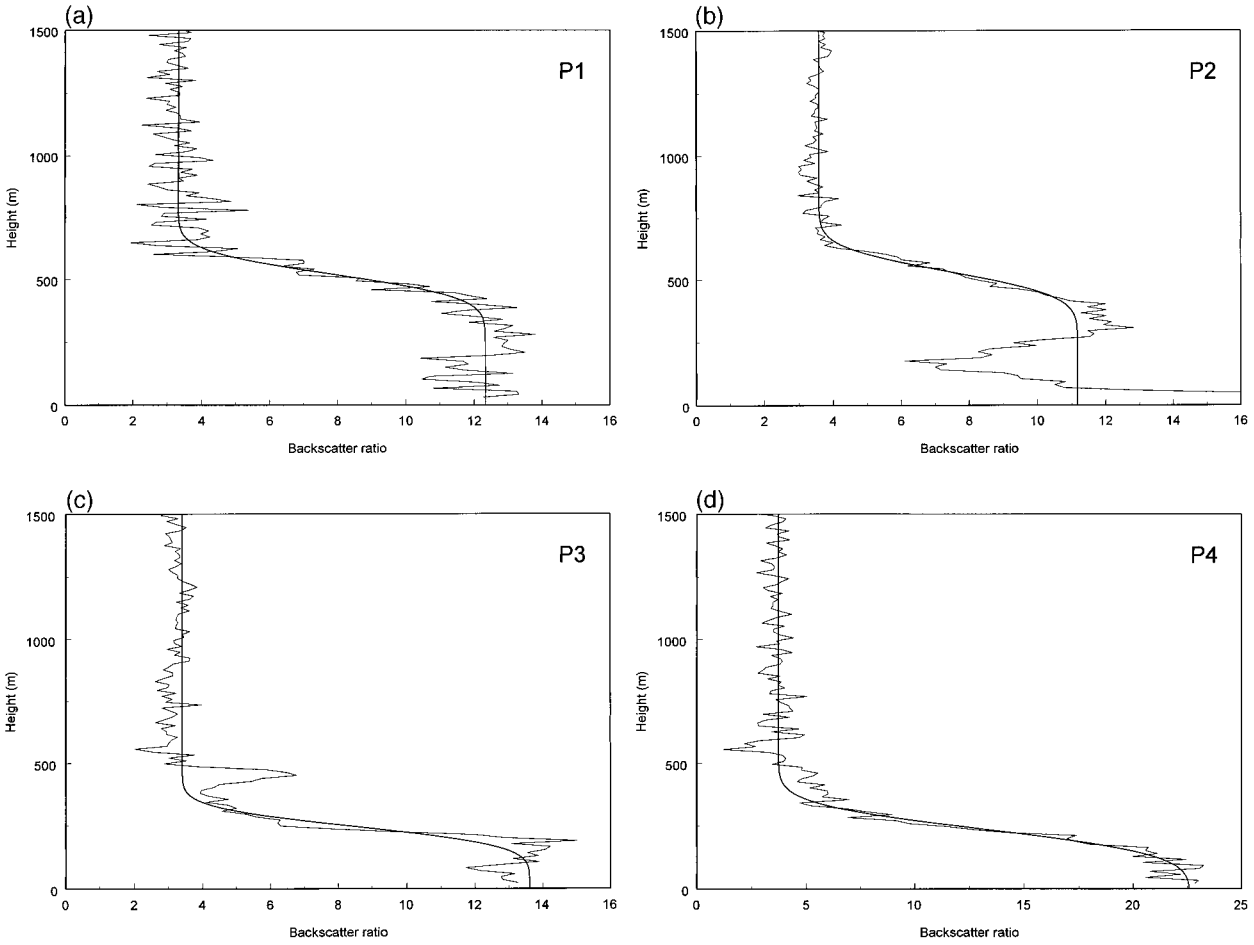

FIG. 2. Observed backscatter profiles listed in Table 1. Smooth line is fitted idealized profile. (a) Profile P1, (b) profile P2, (c) profile P3, and (d) profile P4.

profile displays greater vertical variation than is expected of the ideal mixed layer overlain by relatively clean air. An examination of a two-dimensional plot of backscatter ratio along this flight leg (L9S on 3 Aug 1993) confirms that the mixed layer around latitude 49.0°N is in the range 240–250 m deep. In this case again, the technique easily detects the MLD and manages to avoid the confounding elevated plume.

Profile P4 (Fig. 2d) shows a very shallow mixed layer. The technique has no difficulty in detecting the MLD in this case, in spite of the very shallow mixed layer. From Figs. 2a–d it is evident that the noise component (loosely defined as deviations from the idealized fitted profile) has a peak-to-peak amplitude of roughly 1.5 in backscatter ratio.

In addition to listing profile identification information, Table 1 lists the fitted parameters (z_m, s, B_u, and B_m) as well as MLD detected by other techniques for comparison. Here, z_{m1} and z_{m2} are MLD determined by critical backscatter, the upper height is the first height at which backscatter equals the critical value when scanning the profile downward, and the lower height is for upward scanning. In this case, the critical backscatter was determined by subjectively averaging mixed layer and upper layer backscatter and taking the average of the resulting values. In all cases, the MLD detected by the present technique falls between z_{m1} and z_{m2}. Invariably, the difference between z_{m1} and z_{m2} is greater than s, and an unacceptably large fraction of z_m. Also, z_{md} is MLD detected by the derivative of backscatter. This detection is based on an analysis of the profiles after smoothing with a five point moving average. In the case of P1, it agrees quite well with z_m, but in the more difficult examples, the technique fails to detect a MLD, or detects an obviously incorrect value. Table 1 also shows the minimized value of rmsd (in backscatter ratio) between fitted and measured profile. The values of rmsd are consistent with the observation that the peak-to-peak amplitude is roughly 1.5 in backscatter ratio.

The method of finding the best fit profile optimizes all four parameters simultaneously by minimization of the rmsd between observed and ideal profiles. Since z_m and s have more significant physical meaning than B_u and B_m, it is useful to examine the behavior of the

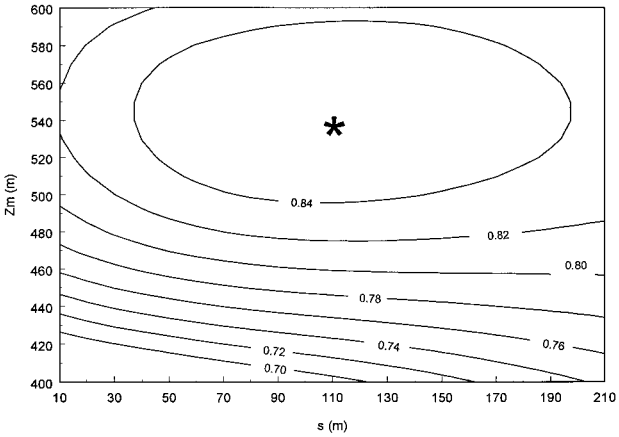

FIG. 3. Contours (in z_m–s space) of the coefficient of linear correlation (r^2) between $b(z)$ and $B(z)$ with fixed values $B_u = 4.0$, and $B_m = 11.0$ for observed backscatter profile P2 listed in Table 1. Asterisk indicates the values of in z_m and s determined by multidimensional minimization.

coefficient of linear correlation (r^2) between observed and ideal profiles for a range of values of z_m and s. Profile P2 is used in this exercise. Values of B_u and B_m are set at 3.578 and 11.171 (from Table 1), respectively, and r^2 is contoured for the parameter range $10.0 < s < 210.0$ and $400.0 < z_m < 600.0$. From Fig. 3 it is clear that the optimization (in these two parameters at least) should be fairly straightforward since the function is smoothly varying. It is also clear that z_m will be much more robustly determined than s since gradients in s are very small.

b. Testing with synthetic profiles

In order further to test the technique, a set of synthetic backscatter profiles (F1–F3) was developed. The profiles are constructed by adding a random noise component to an analytic component. The random noise is a normally distributed sequence with zero mean and a standard deviation of 1.0. This is taken as a typical value, based on observed peak-to-peak amplitude (1.5) of the observed profiles as well as rmsd (0.75) for the fitted profiles. For profiles F1 and F2, the analytic component has B_m equal to 10.0, with B_u of 2.0 (for F1) and 8.0 (for F2). The intent of this pair of profiles is to investigate if the technique is able to detect MLD and EZT when the backscatter contrast between mixed layer air and overlying air becomes small. A third synthetic profile is constructed by adding two layers of backscatter ratio 5.0 units to profile F1. The layers are at 150.0 to 250.0 m, and 860.0 to 960.0 m. All synthetic profiles are specified at 10-m vertical intervals. Profiles F1 to F3 are plotted on Figs. 4a–c, and their parameters are listed in Table 2.

Judging by Table 2, and Figs. 4a–c, the technique has no difficulty in detecting both MLD and EZT, even in the two very difficult cases represented by profiles F2 and F3. In profile F3, the two fitted backscatter levels are obviously larger than the analytical ones because of the influence of the strongly scattering layers. It is also clear in this case that the MLD has been underestimated and EZT overestimated because of the influence of the structure in the mixed layer.

c. X–Z section

In order to investigate the feasibility of automated operation of this technique, a sequence of profiles was extracted from the Pacific '93 lidar dataset. A section of flight leg L07N on 5 August 1993 containing 72 profiles was analyzed, and the results displayed in Fig. 5 as latitude–height sections of topography, MLD and EZT. EZT is plotted as a band of width 2.77s centered on the MLD. The analyses consisted of a simple sequential application of the MLD detection algorithm without any horizontal (multiple profile) or vertical (within profile) averaging. The optimization algorithm performed flawlessly, achieving convergence for all 72 profiles and producing a pattern of MLD and EZT that is entirely consistent with similar patterns examined by Davis et al. (1997). Melfi et al. (1985) show that the ratio of inversion base entrainment heat flux to surface layer heat flux can be estimated from MLD and EZT. It can be shown that their ratio is equivalent to

$$\frac{Q_{Hi}}{Q_{Hs}} = \left(\frac{z_m}{1.38s} - 1\right)^{-1}.$$

The mean value of this ratio over all 72 backscatter profiles in Fig. 5 is 0.21, very close to the value of 0.20 used in most slab models of mixed layer growth.

4. Discussion and conclusions

This work has developed a new technique for extracting MLD and EZT from lidar backscatter profiles. The method is based on the fitting of an idealized profile (based on the error function) to the measured backscatter profile. MLD and EZT arise naturally from the fitted profile as two of four fitting parameters. Because the technique employs the entire measured profile, rather then a few critical points, it has robustness not found in other techniques. Analysis of four observed profiles and three synthetic profiles shows this robustness, and demonstrates that the technique is able to detect MLD and EZT even in very difficult cases. The most difficult cases being ones in which mixed layer and upper layer backscatter differ only very slightly, or ones containing plumes of strongly scattering air in mixed and upper layers.

It is important to recognize that the technique presented and tested in this work is designed to detect mixed layers that have a lidar backscatter profile conforming to the ideal of uniform backscatter in, and above the mixed layer, with a relatively sharp transition be-

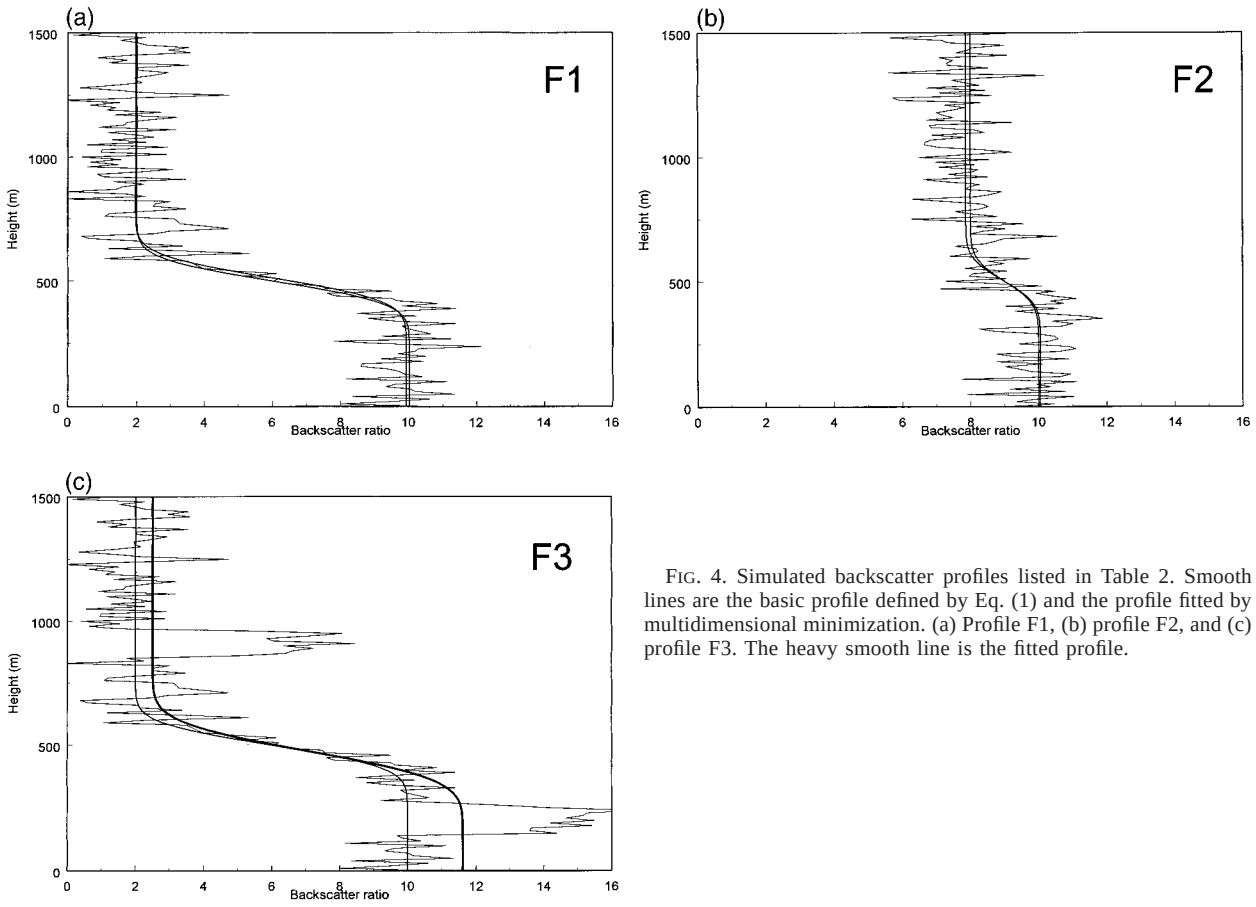

FIG. 4. Simulated backscatter profiles listed in Table 2. Smooth lines are the basic profile defined by Eq. (1) and the profile fitted by multidimensional minimization. (a) Profile F1, (b) profile F2, and (c) profile F3. The heavy smooth line is the fitted profile.

tween these layers. An extensive set of tests (Hägeli 1998) not presented here shows that, in cases where clear air is entrained from above the mixed layer to very near the surface, the method does indicate a very deep EZT, often comparable in depth to the MLD. It is doubtful whether in these transient cases, MLD and EZT are well defined. The technique as presented would not be able to detect MLD in cases of clean, near-surface air overlain by aerosol laden air. Furthermore, the technique can only detect boundary layer structures in the presence of aerosols as tracers, or targets for lidar backscatter.

The robustness of the technique is demonstrated by applying it to a sequence of backscatter profiles. The success of this application shows that the prospect for automated implementation is very good. This has only been possible in the past for highly smoothed profiles, and even then, lack of robustness has resulted in the need for subjective post analysis of MLD time series or spatial sequences. EZT–MLD relationships detected by the present technique are shown to conform to theoretical limits required by entrainment energetics.

Acknowledgments. Data were drawn from parts of the Pacific '93 field study funded by Environment Canada. The work was funded by grants awarded by the Atmospheric Environment Service of Environment Canada and the Natural Science and Engineering Research Council of Canada. MB was able to participate through funding from the NATO–CNR senior fellowships program.

TABLE 2. Synthetic profiles. Here, B_u, B_m, z_m, and s are defined in Eq. (1). The first set of values are used to define the idealized profile, the second set are those determined by the optimization technique. Also, σ is the standard deviation of a random noise component added to the "pure" synthetic profile and f is root-mean-square deviation between synthetic backscatter profile and fitted profile.

Profile	B_u	B_m	z_m (m)	S (m)	σ	B_u	B_m	z_m (m)	s (m)	f
F1	2.0	10.0	500	100	1.0	1.969	9.911	513	102	1.022
F2	8.0	10.0	500	100	1.0	7.859	10.057	502	100	0.988
F3 (plumes)	2.0	10.0	500	100	1.0	2.518	11.613	476	127	1.845

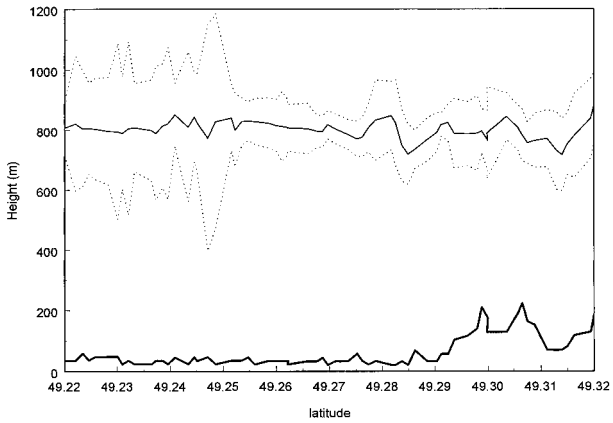

FIG. 5. The *X–Z* section of topography (heavy solid line), mixed layer depth (light solid line) and entrainment layer (dotted line) for flight leg L07N on 5 Aug 1993.

REFERENCES

Batchvarova, E., D. G. Steyn, X. Cai, S.-E. Gryning, and M. Baldi., 1997: Modelling the internal boundary layer in the Lower Fraser Valley, B.C. *Proc. EURSAP Workshop on the Determination of the Mixing Height—Current Progress and Problems,* Risoe, Denmark, EURSAP, 141–144.

Boers, R., E. W. Eloranta, and R. L. Coulter, 1984: Lidar observations of mixed layer dynamics: Tests of parameterized entrainment models. *J. Climate Appl. Meteor.,* **23,** 247–266.

Cohn, S. A., C. J. Grund, S. D. Mayor, and W. M. Angevine, 1997: Boundary layer height and vertical velocity measurements at LIFT. Preprints, *12th Symp. on Boundary Layers and Turbulence,* Vancouver, BC, Canada, Amer. Meteor. Soc., 5–6.

Endlich, R. M., F. Ludwig, and E. E. Uthe, 1979: An automated method for determining the mixing depth from lidar observations. *Atmos. Environ.,* **13,** 1051–1056.

Davis, K. J., D. H. Lenschow, S. P. Oncley, C. Kiemle, G. Ehret, A. Giez, and J. Mann, 1997: Role of entrainment in surface–atmosphere interactions over the boreal forest. *J. Geophys. Res.*, **102,**(D24) 29 219–29 230.

Driedonks, A. G. M., and H. Tennekes, 1984: Entrainment effects in the well-mixed atmospheric boundary layer. *Bound.-Layer Meteor.,* **30,** 75–105.

Hägeli, P., 1998: Evaluation of a new technique for extracting mixed layer depth and entrainment zone thickness from lidar backscatter profiles. Diploma thesis, Swiss Federal Institute of Technology, 71 pp. [Available from Atmospheric Science Programme, University of British Columbia, Vancouver, BC V6T 1Z2, Canada.

Hayden, K. L., K. G. Anlauf, R. M. Hoff, and W. J. Strapp, 1994: PACIFIC '93 Lower Fraser Valley oxidants study aircraft data report. Environment Canada Report, 268 pp.

——, and Coauthors, 1997: The vertical chemical and meteorological structure of the boundary layer in the Lower Fraser Valley during PACIFIC '93. *Atmos. Environ.,* **31** (4), 2089–2106.

Hoff, R. M., L. Guise-Bagley, R. M. Staebler, H. A. Wiebe, J. Brook, B. Georgi, and T. Dusterdiek, 1996: Lidar, nephelometer and and in-situ aerosol experiments in Southern Ontario. *J. Geophys. Res.,* **19** (D10), 199–209.

——, M. Harwood, A. Sheppard, F. Froude, B. A. Martin, and W. Strapp, 1997: Use of airborne lidar to determine aerosol sources and movement in the Lower Fraser Valley (LFV), British Columbia. *Atmos. Environ.,* **31** (4), 2123–2134.

Lenschow, D. H., 1986: *Probing the Atmospheric Boundary Layer.* Amer. Meteor. Soc., 269 pp.

Melfi, S. H., J. D. Spinhire, S.-H. Chou, and S. P. Palm, 1985: Lidar observation of vertically organized convection in the planetary boundary layer over the ocean., *J. Climate Appl. Meteor.,* **24,** 806–821.

Nelson, E., R. Stull, and E. Eloranta, 1989: A prognostic relation for entrainment zone thickness. *J. Appl. Meteor.,* **28,** 885–903.

Pottier, J., B. Thomson, J. Bottenheim, and D. G. Steyn, 1994: Lower Fraser Valley oxidants study and Pacific '93 meta data report. Canadian Institute for Research in Atmospheric Chemistry Report, 50 pp.

Press, W. H., S. A. Teukolsky, W. T. Vettering, and B. R. Flannery, 1992: *Numerical Recipes in FORTRAN: The Art of Scientific Computing.* 2d ed. Cambridge University Press, 963 pp.

Steyn, D. G., J. W. Bottenheim, and R. B. Thomson, 1997: Overview of tropospheric ozone in the Lower Fraser Valley, and the PACIFIC '93 field study. *Atmos. Environ.,* **31** (4), 2025–2136.

Stull, R. B., 1988: *An Introduction to Boundary Layer Meteorology.* Kluwer Academic Publishers, 666 pp.